Air Force Institute of Technology

AFIT Scholar

Faculty Publications

11-25-2019

Gamma-ray Radiation Effects in Graphene-based Transistors with h-BN Nanometer Film Substrates

E. J. Cazalas
University of Utah

Michael R. Hogsed

S. R. Vangala
Air Force Research Laboratory

Michael R. Snure
Air Force Research Laboratory

John W. McClory
Air Force Institute of Technology

Follow this and additional works at: https://scholar.afit.edu/facpub

Part of the Electrical and Electronics Commons, Nanoscience and Nanotechnology Commons, and the Nuclear Commons

Recommended Citation

Cazalas, E. J., Hogsed, M. R., Vangala, S., Snure, M. R., & McClory, J. W. (2019). Gamma-ray radiation effects in graphene-based transistors with h-BN nanometer film substrates. Applied Physics Letters, 115(22), 223504. https://doi.org/10.1063/1.5127895

This Article is brought to you for free and open access by AFIT Scholar. It has been accepted for inclusion in Faculty Publications by an authorized administrator of AFIT Scholar. For more information, please contact richard.mansfield@afit.edu.

Applied Physics Letters

Gamma-ray radiation effects in graphene-based transistors with h-BN nanometer film substrates

Cite as: Appl. Phys. Lett. **115**, 223504 (2019); https://doi.org/10.1063/1.5127895
Submitted: 15 September 2019 . Accepted: 11 November 2019 . Published Online: 26 November 2019

E. Cazalas, M. R. Hogsed, S. Vangala, M. R. Snure, and J. W. McClory

View Online

Export Citation

CrossMark

ARTICLES YOU MAY BE INTERESTED IN

Thermal droop in high-quality InGaN LEDs
Applied Physics Letters **115**, 223502 (2019); https://doi.org/10.1063/1.5124123

Transmorphic epitaxial growth of AlN nucleation layers on SiC substrates for high-breakdown thin GaN transistors
Applied Physics Letters **115**, 221601 (2019); https://doi.org/10.1063/1.5123374

High-performance all-solution-processed quantum dot near-infrared-to-visible upconversion devices for harvesting photogenerated electrons
Applied Physics Letters **115**, 221103 (2019); https://doi.org/10.1063/1.5124735

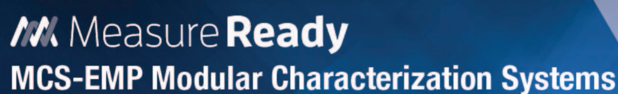

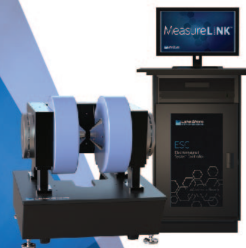

NEW
Multi-purpose platforms for
automated variable-field experiments
Find out more

AIP Publishing

© 2019 Author(s).

Applied Physics Letters ARTICLE scitation.org/journal/apl

Gamma-ray radiation effects in graphene-based transistors with h-BN nanometer film substrates

Cite as: Appl. Phys. Lett. **115**, 223504 (2019); doi: 10.1063/1.5127895
Submitted: 15 September 2019 · Accepted: 11 November 2019 ·
Published Online: 26 November 2019

View Online

Export Citation

CrossMark

E. Cazalas,[1,2,a] M. R. Hogsed,[1] S. Vangala,[3] M. R. Snure,[3] and J. W. McClory[1]

AFFILIATIONS

[1]Department of Engineering Physics, Air Force Institute of Technology, Wright-Patterson Air Force Base, Ohio 45433, USA
[2]Nuclear Engineering Program, Department of Civil and Environmental Engineering, University of Utah, Salt Lake City, Utah 84112, USA
[3]Sensors Directorate, Air Force Research Laboratory, Wright-Patterson Air Force Base, Ohio 45433, USA

[a]Author to whom correspondence should be addressed: edward.cazalas@utah.edu

ABSTRACT

Radiation effects on graphene field effect transistors (GFETs) with hexagonal boron nitride (h-BN) thin film substrates are investigated using ^{60}Co gamma-ray radiation. This study examines the radiation response using many samples with varying h-BN film thicknesses (1.6 and 20 nm thickness) and graphene channel lengths (5 and 10 μm). These samples were exposed to a total ionizing dose of approximately 1 Mrad(Si). I-V measurements were taken at fixed time intervals between irradiations and postirradiation. Dirac point voltage and current are extracted from the I-V measurements, as well as mobility, Dirac voltage hysteresis, and the total number of GFETs that remain properly operational. The results show a decrease in Dirac voltage during irradiation, with a rise of this voltage and permanent drop in Dirac current postirradiation. 1.6 nm h-BN substrate GFETs show an increase in mobility during irradiation, which drops back to preirradiation conditions in postirradiation measurements. Hysteretic changes to the Dirac voltage are the strongest during irradiation for the 20 nm thick h-BN substrate GFETs and after irradiation for the 1.6 nm thick h-BN GFETs. Failure rates were similar for most GFET types during irradiation; however, after irradiation, GFETs with 20 nm h-BN substrates experienced substantially more failures compared to 1.6 nm h-BN substrate GFETs.

Published under license by AIP Publishing. https://doi.org/10.1063/1.5127895

Interest in graphene-based field effect transistor (GFET) research has increased with investigations into integrated circuit, sensor, and memory device applications.[1] A challenging aspect of using GFETs is their sensitivity to small changes in the local electric field, which can drastically affect the current-voltage (I-V) characteristics of the GFET.[2] These changes in the local electric field are typically due to interactions with the neighboring substrate and may include environmental changes (such as humidity)[3] or exposure to visible light and ionizing radiation.[4–7] The substrate on which the graphene device resides can play an important role in graphene's reactivity with the environment,[8] charge carrier density and mobility,[9] and thermal properties.[10] Hexagonal boron nitride (h-BN) has been identified as a promising substrate or passivating layer due to being atomically smooth, relatively free of dangling bonds, and having a lattice constant similar to graphite.[11]

Atomically thin graphene is an interesting candidate for utilization in radiation hardened or resilient devices as it presents a small volume for radiation interaction; yet, the graphene layer is sensitive to local environmental conditions that may be modified by irradiation. One interesting application area for GFETs is in developing radiation resilient electronics for high flux ionizing radiation fields, such as in space,[12] where the utilization of h-BN may be especially advantageous. Here, we present the investigation of the radiation effects of the total ionizing dose (TID) on top-gated GFETs that utilize nanometer thick h-BN substrates on crystalline Al_2O_3 (sapphire) with an Al_2O_3 gate oxide. This investigation adds to the existing body of work that explores radiation effects on carbon-based devices.[13–19]

We examine the modification of I-V characteristics, including the shift in the charge neutrality point in terms of applied gate voltage (V_{sg}) and measured source current (I_{sd}). The changes in the charge neutrality point or Dirac point in terms of voltage (Dirac voltage, V_d) and current (Dirac current, I_d) due to gamma-ray radiation for GFETs utilizing various h-BN thicknesses and graphene channel lengths (L_{ch}) are of primary interest in this study along with changes in mobility and Dirac voltage hysteresis. In addition to monitoring modifications to I-V characteristics, we also track the radiation induced failure of

Published under license by AIP Publishing

many GFETs. The change in I-V characteristics and GFET survival is conducted at TID levels of Mrad(Si) order using a ^{60}Co gamma-ray source.

The GFETs were produced by the Air Force Research Laboratory by growing CVD h-BN onto sapphire substrates.[20] The substrate consists of 350 μm of sapphire with h-BN of thickness 1.6 or 20 nm (roughness ~0.1 and 1 nm, respectively) at the graphene interface. Transferred CVD graphene was supplied by Graphenea[21] and top-gated transistor structures were formed, as in the profile view in Fig. 1(a). The top-gate consists of Ni/Au (50/300 nm) with the source, drain, and gate contacts consisting of Ti/Pt/Au (20/30/250 nm). A 20 nm thick layer of aluminum oxide makes up the gate oxide, which also passivates the graphene channel. The graphene channels formed are 150 μm wide with lengths of either $L_{ch} = 5$ or 10 μm. A table in Fig. 1 shows labeling of the devices used in this paper and their h-BN thickness and channel length. A single GFET is controlled by the gate, source, and drain, with a shared gate and drain contact with another graphene channel, as in the lower portion of Fig. 1. Throughout the experiment, only a single graphene channel was measured for any given pair of GFETs.

Pre- and postirradiation I-V measurements were collected using a Signatone Checkmate Analytic CM220 probe-station along with a Keithley 4200A-SCS analyzer. Measurements were taken in ambient conditions. A Keysight B2902A SMU was used for I-V measurements collected between irradiations. The radiation source for gamma irradiations was the ^{60}Co Gamma Irradiator at the Ohio State University Nuclear Reactor Laboratory with a dose rate of approximately 15.6 krad/h (Si) at the test location for the GFETs.[24] The GFETs were placed into an Al-Pb box, to minimize dose from low-energy scattered gamma-rays (as per MIL-STD-883K[25]).

NanoDot dosimeters (from Landauer) were used to verify the dose at approximately 1 in. intervals as a function of height within the Al-Pb box after the irradiation of the GFETs. Extrapolating dosimeter results, TID of 1.65 and 1.75 Mrad(Si) was delivered to the h-BN thicknesses of 1.6 and 20 nm, respectively, over a span of 4.7 days.

A total of 79 GFETs were evaluated using 498 I-V measurements collected. For this experiment, an I-V measurement was taken before irradiation. Then, TID was delivered over five exposure periods, with the I-V measurement of devices after each exposure period. This procedure closely replicates an *in situ* measurement as the I-V measurements of all the devices were conducted within approximately an hour after an exposure period. Finally, the GFETs were measured at various time intervals postirradiation, up to the final measurement at ~35 days after the final irradiation. In all experiments, no V_{gs} or V_{sd} was applied during irradiation due to the large number of devices.

The measurement procedure involved five consecutive exposures that brought the TID to 1.65 and 1.75 Mrad(Si) for the GFETs with h-BN thicknesses of 1.6 and 20 nm, respectively. Between each exposure, I-V measurements were performed and the changes in V_d and I_d were assessed, as shown in Figs. 2(a) and 2(b). V_d and I_d changes were also assessed using I-V measurements postirradiation, as shown in Figs. 2(c) and 2(d). The exact dose delivered to each set of GFETs during irradiation is given in supplementary material Figs. S1–S4.

The Dirac voltage represents the point of the lowest Dirac current in the I-V measurements. The Dirac voltage was taken for the forward voltage sweep direction of the I-V curve. The Dirac voltage shows a drop after initial irradiation, in Figs. 2(a) and 2(c), with a more substantial change for the GFETs with a channel length of $L_{ch} = 5$ μm. The Dirac voltage remains depressed during irradiation. After irradiation, the GFETs show an increase in Dirac voltage above their initial voltages, again with a more substantial change for the $L_{ch} = 5$ μm GFETs. The Dirac currents show a slight increase during irradiation, in Fig. 2(c), with a return toward their initial currents preirradiation in postirradiation measurements in Fig. 2(d).

The charge carrier mobility is given preirradiation and during irradiation in Fig. 3(a). Mobility postirradiation is shown in Fig. 3(b). The mobility was calculated from the I-V measurements by using the transconductance methods of the forward sweep for the electron side

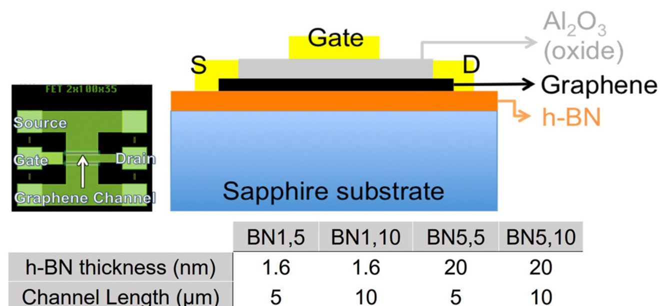

	BN1,5	BN1,10	BN5,5	BN5,10
h-BN thickness (nm)	1.6	1.6	20	20
Channel Length (µm)	5	10	5	10

FIG. 1. The h-BN based GFET architecture has been previously tested and show improvements, such as decreased carrier density and increased mobility, over graphene on sapphire.[22] Measurements are made by the application of a source-drain voltage (V_{sd}) with a gate voltage (V_g) used to modulate carriers in graphene. The table below shows labels used for devices of different channel lengths and h-BN thicknesses in this paper. Adapted from J. F. Brickey, Master's thesis (Air Force Institute of Technology, WPAFB, OH, 2018).[23]

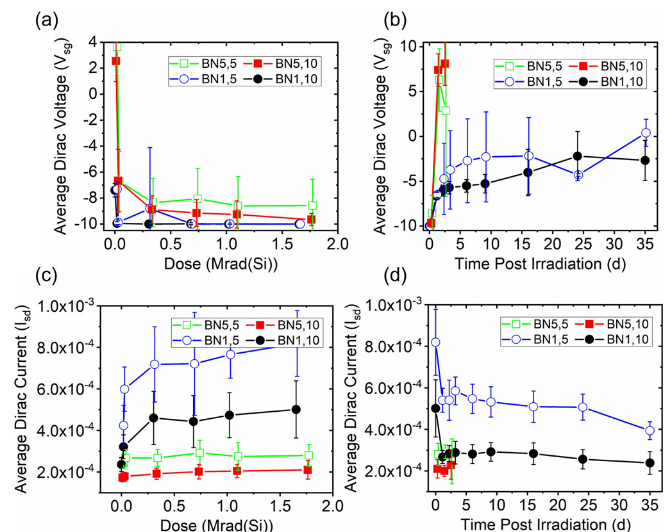

FIG. 2. The I-V characteristics of the GFETs (a) during irradiation (preirradiation measurement taken at zero dose) and (b) postirradiation measurements after TID of 1.65 and 1.75 Mrad(Si) was delivered to the h-BN thickness of 1.6 and 20 nm, respectively. The Dirac currents of the GFETs (c) during irradiation and (d) postirradiation are also shown. The last data point in (a) and (c) corresponds to the first data point in (b) and (d). Data points were slightly offset from true x-axis values to prevent the overlap of data points and error bars.

Published under license by AIP Publishing

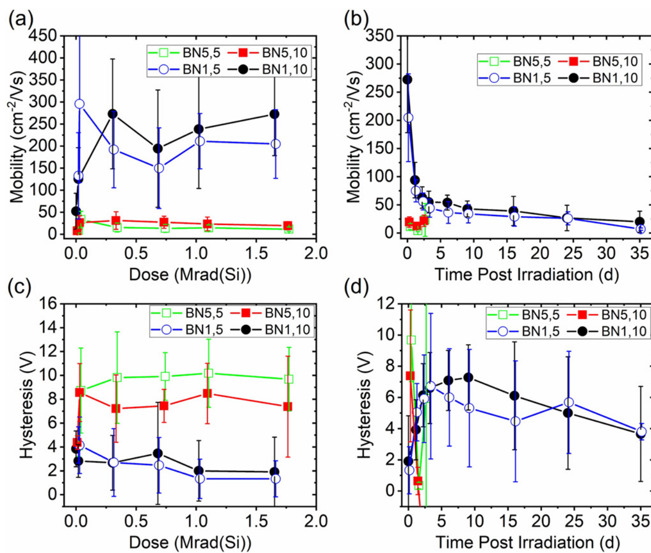

FIG. 3. The charge carrier mobility (a) during irradiation (preirradiation measurement taken at zero dose) and (b) postirradiation measurements after TID of 1.65 and 1.75 Mrad(Si) was delivered to the h-BN thickness of 1.6 and 20 nm. The hysteresis of the Dirac voltage of the GFETs (c) during irradiation and (d) postirradiation is also shown. The last data point in (a) and (c) corresponds to the first data point in (b) and (d). Data points were slightly offset from true x-axis values to prevent the overlap of data points and error bars.

of the Dirac point. Mobilities for the h-BN thickness of 20 nm were always lower than those for the 1.6 nm thickness and remained nearly unchanged during and postirradiation, with an increase during irradiation for the 1.6 nm thickness devices. During irradiation, the 1.6 nm thick devices show an increase and sustainment of mobility, in Fig. 3(a), and then a decrease back to preirradiation mobilities in postirradiation measurements, in Fig. 3(b).

The hysteresis of the Dirac voltages was calculated from the I-V measurements. The hysteresis is the difference in the Dirac voltage point for the backward voltage sweep direction vs the forward voltage sweep direction ($V_{d,-} - V_{d,+}$). The hysteresis is shown in Figs. 3(c) and 3(d), which is always positive, indicating that the Dirac voltages for the backward sweep are greater than those for the forward sweep, as expected.[26] The hysteresis for all devices remained relatively unchanged during irradiation but increased for the 1.6 nm thick h-BN devices in postirradiation measurements.

The fractional number of operational GFETs (exhibit source-drain currents within an order of magnitude of preirradiation measurements) was tracked during and postirradiation, shown in Figs. 4(a) and 4(b), respectively. It is noted that GFET failure modes of source-drain current drift and abrupt failure or destruction were observed. In Figs. 3(a) and 3(b), preirradiation measurements were taken and are shown at dose = 0 [also the case in Fig. 4(a)].

Initial Dirac voltage, V_d, for all GFET types with a h-BN thickness of 1.6 nm shows n-doping of graphene, as shown in Fig. 2(a) (time = 0 d), while 20 nm thick h-BN devices show p-doping, apparent due to the negative and positive value of the Dirac voltage. The n-type doping in the 1.6 nm h-BN thick samples is consistent with previous Hall effect test structure measurements;[20] however, mobility

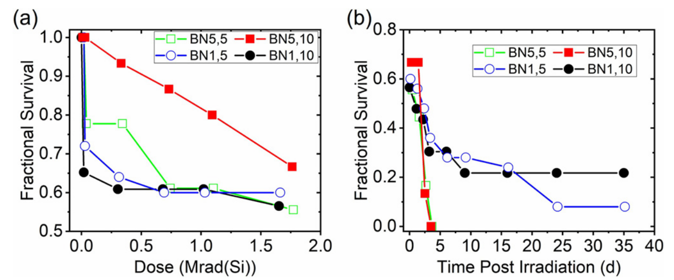

FIG. 4. The fractional number of operational GFETs during (a) irradiation and (b) postirradiation are shown. Data points were slightly offset from true x-axis values to prevent the overlap of data points and error bars. The last data point in (a) corresponds to the first data point in (b).

is substantially poorer compared to these previous measurements, possibly due to contact resistance. The initial V_d is highly dependent on the presence of impurities (H_2O and O_2) at the graphene/Al_2O_3 interface. Additionally, the naturally p-doped graphene on h-BN will become more n-type doped with the decreasing concentration of impurities.[13]

Irradiation affects GFETs by decreasing the Dirac voltage V_d and increasing current I_d for all GFET types (h-BN thicknesses and channel lengths), as in shown Fig. 2(a). This behavior has been previously observed for GFETs exposed to radiation.[15,16] This behavior is caused by the interaction of gamma-rays in the Al_2O_3 gate oxide, which produces electron-hole pairs. While the electrons are more mobile, the holes become trapped at impurity and defect sites at the graphene/Al_2O_3 interface or within the Al_2O_3 gate oxide itself, causing significant n-type doping of the GFETs.[27] After irradiation, all GFETs show an increase in V_d to above preirradiation voltages, as shown in Fig. 2(b). This "rebound" effect has been previously observed and is thought to be due to the annealing of hole defects in the bulk gate oxide, while electrons remain trapped at the graphene/Al_2O_3 interface, eventually creating a situation where the trapped electrons outnumber the trapped holes.[28]

GFET Dirac current, I_d, shows a slight increase during irradiation, as shown in Fig. 2(c). This behavior has been observed in other similar irradiation studies.[15,16] The cause of this slight increase may be due to increased leakage current through the gate oxide as electrically active defects within the bulk Al_2O_3 are created by irradiation.[29] Once irradiation has stopped, postirradiation I_d, as shown in Fig. 2(d), returns to preirradiation levels for all GFETs, likely as the electrically active defects become neutralized.

Mobility for the 1.6 nm thick h-BN substrate GFETs increases significantly during irradiation, as shown in Fig. 3(a). The mobility of 20 nm thick h-BN GFETs increases slightly during irradiation, compared to the 1.6 nm thick h-BN GFETs. This increase in mobility during irradiation is not expected, as reported in Si/SiO_2-based devices, which show a degradation of mobility when irradiated.[15,16] One possible explanation for this increase in mobility may be dehydrogenation at the interface between the graphene and the h-BN substrate and Al_2O_3 oxide. Irradiation of the bulk sapphire and the h-BN substrate creates electron-hole pairs, which recombine and diffuse within the electric field free substrate. As described by Zhang *et al.*,[13] holes that become trapped at or very near the graphene/h-BN interface can cause dehydrogenation of that interface. This hydrogen had been graphene

Published under license by AIP Publishing

carrier scattering sites, and their removal increases the charge carrier mobility; however, since these hydrogens provide no electric field screening, their removal does not affect the Dirac voltage or hysteresis. The relative roughness of the 1.6 nm thick h-BN substrate compared to the 20 nm thickness (0.1 nm for h-BN thickness = 1.6 nm vs 1 nm roughness for 20 nm) means that the 1.6 nm thick GFETs would experience a greater effect from dehydrogenation as the graphene is more regular in closer proximity to the h-BN. In postirradiation measurements, as shown in Fig. 3(b), the mobility drops over time for the 1.6 nm thick h-BN GFETs, likely as the graphene/h-BN interface hydrogenates back to preirradiation levels.

Hysteresis measurements during irradiation show opposite trends for 1.6 nm thick GFETs, which slightly decreased compared to the preirradiation measurement, and 20 nm thick GFETs, which increased compared to preirradiation measurements, shown in Fig. 3(c). Again, opposite trends are observed in the hysteresis of postirradiation measurements for 1.6 vs 20 nm thick GFETs, shown in Fig. 3(d). One known cause of hysteresis is the redox reaction of H_2O and O_2 species at the graphene/Al_2O_3 gate oxide interface that is driven by the gate-graphene electric field.[29] The apparently opposite trends of 1.6 vs 20 nm thick GFET hysteresis reflect an artifact of the measurement. We observe that Dirac voltage becomes highly negative for both h-BN thickness GFETs, as shown in Fig. 1(a). However, the 1.6 nm thick h-BN GFETs reach the minimum limit of the measurement range at $V_{gs} = -10$ V, while the 20 nm thick h-BN did not. For this reason, the magnitude of the hysteresis is measured as smaller for the 1.6 nm h-BN GFETs only because the forward sweep Dirac point must take on the range limit, $V_{d,+} = V_{gs} = -10$ V, and thus, the full difference in the hysteresis, $V_{d,-} - V_{d,+}$, is not fully expressed or truncated by the measurement range. Postirradiation measurements of 1.6 nm h-BN show an increase and recovery of the hysteresis toward the preirradiation measurement. This is due to the annealing of trapped charges in the oxide and at the graphene/oxide interface (responsible for the recovery) and the recovery of the forward sweep Dirac voltage back into the range of measurement (responsible for the perceived rise in hysteresis). It is believed that if a larger measurement range that fully measured the Dirac voltages were implemented, the trend of the 1.6 nm h-BN GFETs would follow that observed for the 20 nm h-BN GFETs.

The fractional survival of GFETs during irradiation generally shows a drop in functional GFETs due to irradiation after the first irradiation session [delivered dose of 20 krad(Si)], as shown in Fig. 4(a). The cause of failure during irradiation may be due to the introduction of radiation induced trapped charges at the graphene/oxide interface and in the bulk oxide, which can lead to increased leakage current.[30] In postirradiation measurements, a further reduction in the fractional survival of GFETs is immediately observed, as shown in Fig. 4(b). This may be due to the rehydrogenation of the graphene/h-BN surface and annealing of trapped charges at the graphene/oxide interface and in the bulk oxide, increasing carrier scattering, and Joule heating of graphene.[31,32] It is likely that the higher failure rate of the 20 nm h-BN GFETs was due to higher graphene roughness, making them more susceptible to Joule heating failure.[33]

TID effects on GFETs of different thicknesses of h-BN substrates and different graphene channel lengths were investigated by analyzing I-V data and device failure rates when irradiated up to a gamma-ray dose of 1.75 Mrad(Si). The results show a decrease in the Dirac voltage during irradiation and recovery in postirradiation, while Dirac currents increased during irradiation and recovered postirradiation for all GFET types. These effects were likely due to the introduction of radiation induced trapped charges in the bulk oxide and at the graphene/oxide interface. An increase in mobility was observed for GFETs with 1.6 nm h-BN substrates, which recovers postirradiation. This increase in mobility is proposed to be due to dehydrogenation at the graphene/h-BN interface, reducing carrier scattering. The failure of the devices increased after the first irradiation session [delivered dose of 20 krad(Si)] and then immediately in postirradiation measurements with the GFETs with a 20 nm h-BN substrate having a much higher failure rate, likely due to higher graphene roughness in these GFETs, making them more susceptible to Joule heating failure.

Compared to other GFET structures that utilize more traditional substrates (SiO_2 and/or Si), the change in Dirac voltage for the h-BN-based GFET structure studied here was on par or smaller,[14,15,32] except for that reported by Esqueda *et al.*[16] and Zhang *et al.*,[13] which also utilized a h-BN substrate. Notably, the mobility of our GFET structure exhibited an increase during irradiation, which is opposite to that reported for any other GFET device structures reported.[13–16,33] This investigation provides potentially valuable results to those interested in fabricating radiation resilient GFETs with h-BN and understanding of the effects of TID on GFETs based on h-BN substrates.

See the supplementary material for additional information of I-V characteristics before, during, and after irradiation provided in the plots.

The authors would like to thank the staff of the Ohio State University Nuclear Reactor Laboratory for their support of this research. This work was supported at the Air Force Institute of Technology by the Air Force Research Laboratory Sensors Directorate, AFRL/RYDH. The work done at AFRL was funded by the Air Force Office of Scientific Research under Award No. FA9550-16RYCOR331. Views expressed in this paper are those of the authors and do not necessarily reflect the official policy or position of the Air Force, the Department of Defense, or the United States Government.

REFERENCES

1. E. P. Randviir, D. A. C. Brownson, and C. E. Banks, "A decade of graphene research: Production, applications and outlook," Mater. Today **17**, 426–432 (2014).
2. D. Chen, L. Tang, and J. Li, "Graphene-based materials in electrochemistry," Chem. Soc. Rev. **39**(8), 3157–3180 (2010).
3. H. Xu, Y. Chen, J. Zhang, and H. Zhang, "Investigating the mechanism of hysteresis effect in graphene electrical field device fabricated on SiO_2 substrates using Raman spectroscopy," Small **8**(18), 2833–2840 (2012).
4. E. Cazalas, B. K. Sarker, I. Childres, Y. P. Chen, and I. Jovanovic, "Modulation of graphene field effect by heavy charged particle irradiation," Appl. Phys. Lett. **109**(25), 253501 (2016).
5. M. Foxe, G. Lopez, I. Childres, R. Jalilian, A. Patil, C. Roecker, J. Boguski, I. Jovanovic, and Y. P. Chen, "Graphene field-effect transistors on undoped semiconductor substrates for radiation detection," IEEE Trans. Nanotechnol. **11**(3), 581–587 (2012).
6. E. Cazalas, B. K. Sarker, M. E. Moore, I. Childres, Y. P. Chen, and I. Jovanovic, "Position sensitivity of graphene field effect transistors to X-rays," Appl. Phys. Lett. **106**(22), 223503 (2015).
7. B. K. Sarker, E. Cazalas, T. F. Chung, I. Childres, I. Jovanovic, and Y. P. Chen, "Position-dependent and millimeter-range photodetection in phototransistors

Published under license by AIP Publishing

with micrometer-scale graphene on SiC," Nat. Nanotechnol. **12**(7), 668–674 (2017).
[8]Q. H. Wang, Z. Jin, K. K. Kim, A. J. Hilmer, G. L. C. Paulus, C.-J. Shih, M.-H. Ham, J. D. Sanchez-Yamagishi, K. Watanabe, T. Taniguchi *et al.*, "Understanding and controlling the substrate effect on graphene electron transfer chemistry via reactivity imprint lithography," Nat. Chem. **4**, 724–732 (2012).
[9]Z. Hu, D. P. Sinha, J. U. Lee, and M. Liehr, "Substrate dielectric effects on graphene field effect transistors," J. Appl. Phys. **115**, 194507 (2014).
[10]X. Li, B. D. Kong, J. M. Zavada, and K. W. Kim, "Strong substrate effects of Joule heating in graphene electronics," Appl. Phys. Lett. **99**, 233114 (2011).
[11]C. R. Dean, A. F. Young, I. Meric, C. Lee, L. Wang, S. Sorgenfrei, K. Watanabe, T. Taniguchi, P. Kim, K. L. Shepard *et al.*, "Boron nitride substrates for high-quality graphene electronics," Nat. Nanotechnol. **5**, 722–726 (2010).
[12]J. Osborn, E. Deionno, and A. Bushmaker, "Developing nanoelectronics for space systems," Crosslink **12**(1), 22–29 (2011).
[13]C. X. Zhang, B. Wang, G. X. Duan, E. X. Zhang, D. M. Fleetwood, M. L. Alles, R. D. Schrimpf, A. P. Rooney, E. Khestanova, G. Auton *et al.*, "Total ionizing dose effects on hBN encapsulated graphene devices," IEEE Trans. Nucl. Sci. **61**(6), 2868–2873 (2014).
[14]C. Cress, J. J. McMorrow, J. T. Robinson, B. J. Landi, S. M. Hubbard, and S. R. Messenger, "Radiation effects in carbon nanoelectronics," Electronics **1**, 23–31 (2012).
[15]C. Cress, J. G. Champlain, I. S. Esqueda, J. T. Robinson, A. J. Friedman, and J. J. McMorrow, "Total ionizing dose induced charge carrier scattering in graphene devices," IEEE Trans. Nucl. Sci. **59**(6), 3045–3053 (2012).
[16]I. Esqueda, C. D. Cress, T. J. Anderson, J. R. Ahlbin, M. Bajura, M. Fritze, and J.-S. Moon, "Modeling radiation-induced degradation in top-gated epitaxial graphene field-effect-transistors (FETs)," Electronics **2**, 234–245 (2013).
[17]J. Hicks, R. Arora, E. Kenyon, P. S. Chakraborthy, H. Tinkey, J. Hankinson, C. Berger, W. A. de Heer, E. H. Conrad, and J. D. Cressler, "X-ray radiation effects in multilayer epitaxial graphene," Appl. Phys. Lett. **99**, 232102 (2011).
[18]K. Alexandrou, "Ionizing radiation effects on graphene based field effect transistors," Dissertation (Columbia University, New York, 2016).
[19]I. Childres, L. A. Jauregui, M. Foxe, J. Tian, R. Jalilian, I. Jovanovic, and Y. P. Chen, "Effect of electron-beam irradiation on graphene field effect devices," Appl. Phys. Lett. **97**, 173109 (2010).
[20]M. Snure and Q. Paduano, "Growth of hexagonal boron nitride on microelectronic compatible substrates," MRS Proc. **1781**, 1–10 (2015).
[21]See www.graphenea.com for "Graphenea, Cambridge, MA" (2018).
[22]S. Vangala, G. Siegel, T. Prusnick, and M. Snure, "Wafer scale BN on sapphire substrates for improved graphene transport," Sci. Rep. **8**, 8842 (2018).
[23]J. F. Brickey, "Radiation effects in graphene field effect transistors (GFET) on hexagonal boron nitride (hBN)," Master's thesis (Air Force Institute of Technology, WPAFB, OH, 2018).
[24]See https://reactor.osu.edu/gamma-irradiators for "Gamma Irradiators: ^{60}Co Gamma Irradiator, The Ohio State University, Columbus, OH" (2018).
[25]Department of Defense, *Military Specification MIL-STD-883K (W/Change 2), Department of Defense Test Method Standard: Microcircuits* (DOD, 2017).
[26]E. Cazalas, I. Childres, A. Majcher, T.-F. Chung, Y. P. Chen, and I. Jovanovic, "Hysteretic response of chemical vapor deposition graphene field effect transistors on SiC substrates," Appl. Phys. Lett. **103**, 053123 (2013).
[27]T. R. Oldham and F. B. McLean, "Total ionizing dose effects in MOS oxides and devices," IEEE Trans. Nucl. Sci. **50**(3), 483–499 (2003).
[28]J. R. Schwank, P. S. Winokur, P. J. McWhorter, F. W. Sexton, P. V. Dressendorfer, and D. C. Turpin, "Physical mechanism contributing to device 'rebound'," IEEE Trans. Nucl. Sci. **31**(6), 1434–1438 (1984).
[29]N. C. Das, V. Nathan, R. Tallon, and R. J. Maier, "Radiation effects on gate induced drain leakage current in metal oxide semiconductor transistors," J. Appl. Phys. **72**, 4958 (1992).
[30]K. Xi, J. Bi, S. Majumdar *et al.*, Sci. China Inf. Sci. **62**, 222401 (2019).
[31]J.-H. Chen, C. Jang, S. Adam, M. S. Fuhrer, E. D. Williams, and M. Ishigami, "Charged-impurity scattering in graphene," Nat. Phys. **4**, 377–381 (2008).
[32]C. Dukan and Z. Xiao, "On the failure of graphene devices by Joule heating under current stressing conditions," Appl. Phys. Lett. **107**(24), 243505 (2015).
[33]K. Alexandrou, A. Masurkar, H. Edrees, J. F. Wishart, Y. Hao, N. Petrone, J. Hone, and I. Kymissis, "Improving the radiation hardness of graphene field effect transistors," Appl. Phys. Lett. **109**, 153108 (2016).

Published under license by AIP Publishing